Smartphone assisted fieldwork: Towards the digital transition of geoscience fieldwork using LiDAR-equipped iPhones

Stefano Tavani [a,b], Andrea Billi [b,*], Amerigo Corradetti [c], Marco Mercuri [d], Alessandro Bosman [b,e], Marco Cuffaro [b], Thomas Seers [f], Eugenio Carminati [d]

[a] *Dipartimento di Scienze della Terra, dell'Ambiente e delle Risorse, University of Naples, Italy*
[b] *Consiglio Nazionale delle Ricerche, IGAG, Rome, Italy*
[c] *Dipartimento di Matematica e Geoscienze, University of Trieste, Italy*
[d] *Dipartimento di Scienze della Terra, Sapienza University of Rome, Italy*
[e] *Istituto Superiore per la Protezione e la Ricerca Ambientale, ISPRA, Rome, Italy*
[f] *Petroleum Engineering Program, Texas A&M University at Qatar, Doha, Qatar*

Keywords:
Smartphone
Fieldwork
Mapping
Digital transition
Education
Virtual outcrop models

A B S T R A C T

Major advances in smartphones and tablets in terms of their built-in sensors (esp. cameras), available computational power and on-board memory are transforming the role of such devices into the key digital platform around which geological fieldwork is redesigning itself. This digital transition is changing how geoscientists collect and share multimodal-multidimensional field datasets, which can now be readily distributed via standardized exchange formats and online data repositories. The increased accessibility of digital field datasets means that such data products are no longer the sole preserve of geospatial/geoscience specialists, but also students, stakeholders and the general public alike, providing great opportunities for knowledge transfer over the entirety of the research value chain.

In the wake of this digital transition, the geological community has welcomed with enthusiasm and curiosity the introduction during 2020 of a native LiDAR scanner equipped on both the iPad Pro and the iPhone 12 Pro. This scanner offers a potential paradigm shift in digital geological fieldwork and puts these devices at the forefront of smartphone assisted fieldwork. In this work, we review progress in smartphone/tablet assisted geological fieldwork and test the iPhone 12 Pro's effectiveness as a replacement for conventional geological field tools. Specifically, we evaluate the geo-location accuracy of the iPhone's Global Navigation Satellite System (GNSS) receiver, the effectiveness of its inertial measurement unit (IMU) and magnetometer for orientation data collection, its photo-video imaging capabilities, and the performance of the device's newly equipped LiDAR in the field.

We demonstrate that the performance of the iPhone for orientation and raster image data capture is high, being comparable to analog compass-clinometers and reflex/mirrorless cameras. Whilst location error is within the order of a few meters, the level of accuracy and the fast stabilization of the signal means that, beyond survey grade applications, the iPhone's geo-location capabilities are acceptable for most field cases. With regards to the iPhone's built-in LiDAR scanner, it is an excellent tool for depth assisted camera focusing and for casual 3D outcrop sharing, especially for 'soft' applications such as geo-heritage documentation and the production of teaching materials (here we also propose a simple mode of uploading outcrops models in Google Maps). However, the generated 3D models in some cases may be considered overly crude for detailed interrogation, particularly where the fidelity of the surface reconstruction is critical to the analysis (e.g. mesh facet orientation estimation). Based on our review of the evolution of digital field acquisition technologies and on our extensive field testing of the sensor suite integrated within the iPhone 12 Pro, it is clear that the digital transition of geological fieldwork is already mature, whereby smartphone devices have become as indispensable in the field as the geologists' traditional hammer and hand lens.

1. Introduction

Within the geosciences, transformative close-range remote sensing technologies such as LiDAR and digital photogrammetry, are creating ever greater opportunities to document, analyze and interpret geology exposed at the Earth's surface. These developments act as a complement to classical fieldwork approaches, providing a means to efficiently extract quantitative data from rock exposures (Xu et al., 2000; Fernández et al., 2004; Bellian et al., 2005; Pavlis et al., 2010; Bistacchi et al., 2011; Vasuki et al., 2014; De Paor, 2016; Pavlis and Mason, 2017; Corradetti et al., 2021a; Seers et al., 2021). Moreover, such technologies represent valuable tools to improve the accessibility of outcrop data within geoscience education (Carbonell Carrera and Bermejo Asensio, 2017; Whitmeyer et al., 2020; Cawood et al., 2022), and have become instrumental towards the delivery of field courses during the COVID-19 global pandemic crisis (e.g. Tavani et al., 2020a; Bond and Cawood, 2021). In particular, multi-sensor portable devices, such as tablets and smartphones, are providing great opportunities for public engagement within the Earth sciences (e.g. Walker, 2021), and are allowing geoscience practitioners to embrace new, efficient and readily accessible modes of data collection, storage, and sharing (Burchfiel, 2004; Anadu et al., 2020). Many recent articles have indeed emphasized the utility of mobile devices in geoscientific research and education (Pavlis et al., 2010; Whitmeyer et al., 2010; De Paor, 2016; Bursztyn et al., 2017; Walker et al., 2019; Whitmeyer et al., 2019; Glazner and Walker, 2020; Corradetti et al., 2021b). Mobile platforms are becoming an essential part of conventional fieldwork (i.e. field surveying and mapping: e.g. Allmendinger et al., 2017; Novakova and Pavlis, 2019; Whitmeyer et al., 2019), acting as digital notebooks capable of adding metadata (e.g. geotags and photographs) to observations garnered in the field. The ability to document field observations in a more exhaustive fashion using such tools minimizes the need and associated risk related to undertaking multiple visits to remote and poorly accessible locations to collect missing field data.

Until recently, the basic equipment of field geologists included (at the minimum) a fieldbook, cartographic base maps for mapping

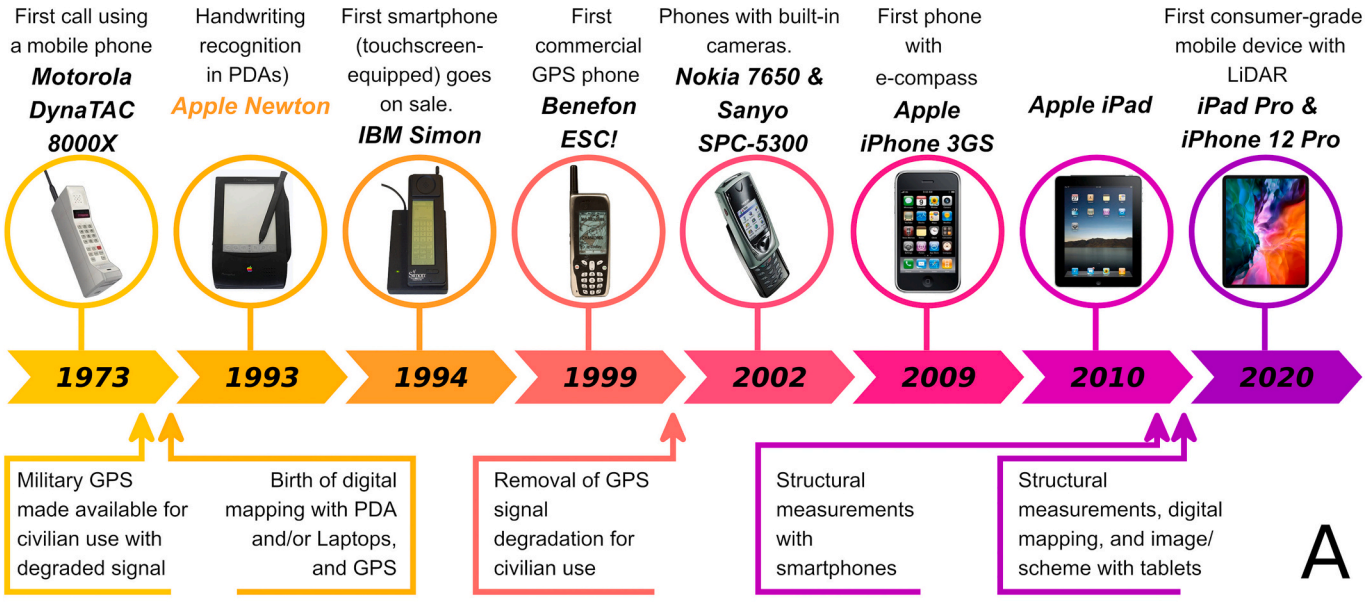

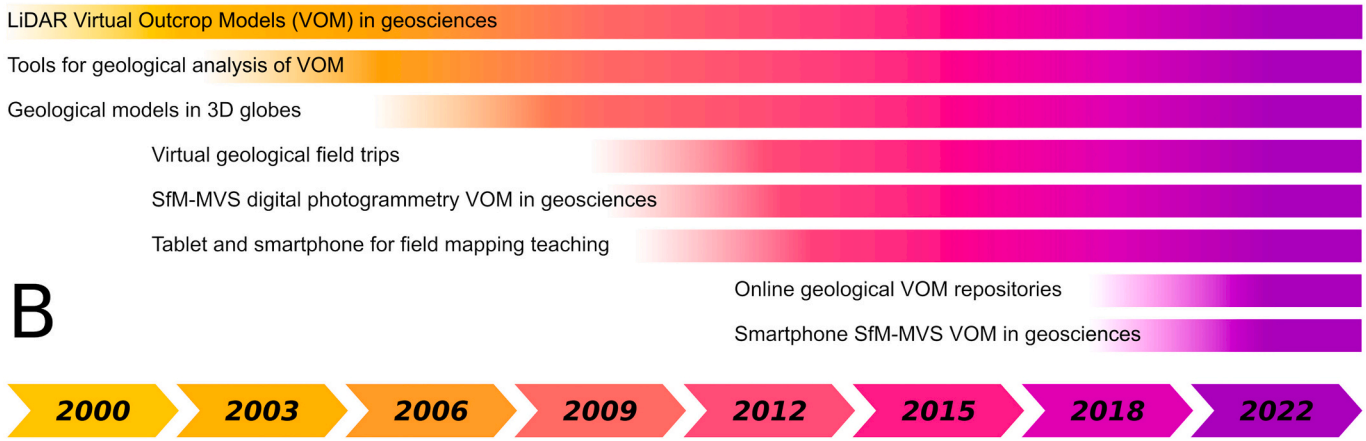

Fig. 1. Chronology of the evolution of digitally assisted fieldwork (A) smartphones and related services presently implemented in them. (B) Scientific progresses in the digital representation and inspection of geological outcrops.

geological observations, a camera for photographic and video documentation, magnifying lenses for rock micro-textural observations, compass-clinometer for structural orientation determination, ruler or tape measure for length measurements (e.g. strata thickness), and geological hammer for sampling. Over the past several decades, rapid technological advancements have led to the replacement or supplementation of many of the aforementioned tools with digital data acquisition systems. Initially, this transition of conventional fieldwork towards digital data capture was facilitated by the introduction of digital cameras, ruggedized laptop computers and handheld global navigation satellite systems (GNSS) (e.g. Carver et al., 1995), and more recently via terrestrial laser scanners/lidars, camera drones and digital compasses. Technological progress in multi-sensor portable devices has consolidated many of these digital tools within tablets and smartphones (Fig. 1A), which are now standard tools within the field geologist's equipment (e.g. Weng et al., 2012; Wolniewicz, 2014; Allmendinger et al., 2017; Novakova and Pavlis, 2019; Lee et al., 2018; Glazner and Walker, 2020; Tavani et al., 2020b; Corradetti et al., 2021b). Expanding the concept of 'primary digital mapping' (McCaffrey et al., 2005), we can now frame smartphone assisted fieldwork as a direct alternative to classical field data collection approaches.

In line with other major developments in personal electronic devices (e.g. touchscreens, built-in cameras, electronic compasses, GNSS receivers etc.), we have recently witnessed what is potentially a major step towards the digitization of geological fieldwork with the release of the LiDAR equipped iPhone 12 Pro (Fig. 1A). This device is the first smartphone equipped with a native LiDAR scanner, capable of capturing 3D scenes directly in the field, offering a potential paradigm shift in digital field data acquisition. Such a capability promises to make outcrop research more repeatable and transparent, providing a means to engage the citizen scientist, and facilitate the exposition of open access, low-cost geospatial data to the general public. Despite the intended core of iPhone LiDAR being the enhancement of digital photo capture (especially low light focusing), its availability has attracted the interest of app developers, resulting in several 3D scanning apps (e.g. 3D Scanner App, Pix4DCatch, Polycam, and EveryPoint), which integrate the iPhone's LiDAR and camera to produce textured 3D scans of decimeter to metre scale scenes. These LiDAR-based software tools form an accompaniment to a diverse set of generic and geologic fieldwork-focused apps used by the geoscientific community, both for research and education. These apps are largely replacing (or have already replaced) the use of standalone digital cameras, notebooks, compasses, and GNSS receivers in the field. The interfaces and sensors that these apps utilize (e.g. touchscreen, camera, magnetometer, gyroscope, GNSS receiver etc.) have been integrated within consumer-grade smartphones for more than a decade, reaching quasi-professional standards within current high-end devices. The iPhone 12 Pro, in particular, is equipped with formidable cameras (12 megapixel front and rear facing) and is capable of a highly efficient stabilization of its magnetometer and GNSS measurements. This makes the iPhone 12 Pro a benchmark system, against which other devices' field performance can be compared.

In this work, we review the key progress in the digital transition of geological fieldwork and detail the capabilities of the iPhone 12 Pro pertinent to field data acquisition. Using primary and published data, we test the capacity of the iPhone 12 Pro to support geological fieldwork in terms of geo-photo, geolocation and digital outcrop data collection, and assess the device's implications towards the development of smartphone assisted fieldwork.

2. Review of previous progress

Over the last three decades, the collection, visualization and analysis of digitized geological data has been largely facilitated by the development of standardized geodatabases, efficiently managed through geographical information systems (GIS). Portable digital devices that enable the collection and analysis of georeferenced field data have been utilized within a small community of geospatial practitioners during the 1990s (e.g. Carver et al., 1995; Brodaric, 1997; Brimhall, 1998; Briner et al., 1999; Kramer, 2000), though such systems have been employed by surveyors and utility workers since the late 1980s (Clegg et al., 2006). Two major technological developments acted as major enablers for digital data collection (Fig. 1A), namely: (1) the availability since the late 1980s of consumer-grade Personal Digital Assistants (PDAs) and portable laptop computers; (2) the authorization during the mid 1980s for the civilian use of the US military's Global Positioning System (GPS, now forming part of a wider GNSS network). Rugged portable PCs, PDAs, and low-cost netbooks, combined with handheld GPS/GNSS receivers are effectively the precursors of modern tablets and smartphones in terms of functionality. Various attempts have been made to utilize these early digital data capture systems to assist geologists in their routine fieldwork (e.g. Brimhall, 1998; Brimhall and Vanegas, 2001; Jones et al., 2004; McCaffrey et al., 2005; De Donatis and Bruciatelli, 2006; Clegg et al., 2006; Pavlis et al., 2010). The introduction of the Apple iPad in 2010 and the subsequent proliferation of similar tablet devices utilizing the Android operating system represented another major step forward in the digitization of fieldwork (e.g. Allmendinger et al., 2017; Novakova and Pavlis, 2019), motivated by the fact that tablets integrated and miniaturized the aforementioned standalone devices into a single low-cost, portable tool. Developments in tablet technology have proceeded in parallel with mobile phones, including the introduction of touchscreens (and the proceeding introduction of high-precision styluses), and the integration of built-in sensors, such as inertial measurement units, magnetometers and GNSS receivers. These developments have been accompanied by gradual increases in computational power, memory, and screen size, as well as major improvements in built-in cameras, resulting in the modern smartphone: the most ubiquitous electronic device in the world today (Fig. 1A).

In 2013, the release of the MidlandValley (now Petroleum Expert) FieldClino app for data collection with smartphones (e.g. Vaughan et al., 2014), with the later release of the FieldMove tablet version in 2015 and of the Strabospot app (Walker et al., 2019; Glazner and Walker, 2020) inaugurated a new era in digital mapping and smartphone assisted fieldwork (e.g. Novakova and Pavlis, 2019). With the availability of these apps and similar geo-focused mobile software tools (e.g. Yeon, 2021), and due to the progressive improvements in hardware functionality, tablets and smartphones have now become robust and diverse field data loggers that are able to digitally record geotagged measurements, field schemes, sketches and photos, whilst acting as a medium for the management of georeferenced maps (e.g. Cawood et al., 2017; Novakova and Pavlis, 2019; Allmendinger et al., 2017). Consequently, tablets and smartphones have become indispensable tools for contemporary fieldwork for many field geologists.

Contemporarily with the increasing capabilities of modern smartphones and tablet, the use of geolocated surface reconstructions (e.g. digital elevation models and virtual outcrop models) produced by geospatial tools and techniques (i.e. close-range digital photogrammetry and LiDAR) increased significantly over the past decade. These tools and their data products are now being routinely employed within both research and educational activities (e.g. Tibaldi et al., 2020; Bond and Cawood, 2021), including geo-heritage site documentation and preservation (e.g. Burnham et al., 2022), geological mapping (e.g. Pavlis and Mason, 2017), outcrop analogue studies for reservoir modelling (e.g. Pringle et al., 2006; Seers and Hodgetts, 2014), seismology (e.g. Hudnut et al., 2002; Bistacchi et al., 2011; Reitman et al., 2015; Corradetti et al., 2021a), sedimentology (e.g. Pringle et al., 2010); structural geology (e.g. Fernández et al., 2004; Bemis et al., 2014), paleontology (e.g. Bates et al., 2008), machine learning (e.g. Sun et al., 2022), volcanology (e.g. Favalli et al., 2010), rockfall detection (van Veen et al., 2017), geomorphology (e.g. Brodu and Lague, 2012), and many other applications within the geosciences. During the late 1990s to early 2000s (Fig. 1B), terrestrial LiDAR revolutionized the study of geological outcrops (e.g. Xu et al., 2000; Pringle et al., 2001; Bellian et al., 2005), permitting high

resolution 3D scans of geological exposures, which when integrated with calibrated photo-imagery, produces colored point clouds or photo-realistic textured triangulated mesh-based reconstructions of rock outcrops (i.e. digital or virtual outcrop models). Subsequent works were aimed at developing algorithms for the interpretation of virtual outcrop models. These works include, among others, the automated/semi-automated extraction of near planar geological surfaces or lineaments from virtual outcrops (e.g. Roncella and Forlani, 2005; Viseur, 2010; García-Sellés et al., 2011; Seers and Hodgetts, 2016), LiDAR signal intensity analysis and/or LiDAR integration with hyperspectral imaging for chemical/lithological interpretation (e.g. Franceschi et al., 2009; Kurz et al., 2011; Hartzell et al., 2014; Penasa et al., 2014), and hypertemporal acquisitions for rock slope monitoring (e.g. Kromer et al., 2015). Despite these efforts, the cost, limited portability and associated learning curve associated with early commercial terrestrial LiDAR systems, limited the use of such tools to a relatively small community of geoscientists. The breakthrough for the widespread use of 3D virtual outcrop models in geosciences has been the application of structure from motion–multiview stereo (SfM-MVS) digital photogrammetry for generating geological surface reconstructions (e.g. James and Robson, 2012; Favalli et al., 2012; Arbués et al., 2012; Bemis et al., 2014; Tavani et al., 2014) (Fig. 1B). Facilitated by the release of open-source and low-cost image processing toolchains (e.g. Bundler: Snavely et al., 2006; PMVS2: Furukawa, 2010; VisualSFM: Wu, 2011), SfM-MVS digital photogrammetry, can be carried out employing consumer-grade digital cameras, foregoing the need for expensive metric cameras and commercial image processing software platforms. The accurate registration of SfM-MVS-derived outcrop reconstructions, however, relies on somewhat poorly portable and relatively expensive tools (e.g. differential GNSS antennas), representing a major limitation for the widespread use of 3D virtual outcrop models. Recently, workers have demonstrated that the improved resolution of smartphone cameras, together with the availability of camera pose information (i.e. position provided by the smartphone's GNSS sensor and orientation provided by the smartphone's magnetometer, gyroscope and accelerometer), makes smartphones amenable to the development of georeferencing schemes for virtual outcrop models without the use of expensive and unwieldy survey-grade differential GNSS receivers (e.g. Tavani et al., 2019). The advent of the LiDAR-equipped iPhone 12 Pro (and the most recent iPhone 13 Pro) and iPad Pro, as well as device supported 3D scanning apps, promises to provide further access to virtual outcrop data capture and analysis for field geologists, negating the need for photo-surveys and photogrammetric scene reconstruction.

In tandem with the progressive development and proliferation of acquisition technologies and virtual outcrop analysis techniques, the adoption of routine geotagging and geospatial data visualization via 3D geo-browsers, such as Google Earth (first release in 2005 after the acquisition of Keyhole, Inc.), has allowed the integration and sharing of photos, texts, hypertextual links and 3D models (including virtual outcrop models) within consolidated platforms (Butler, 2006; Chen et al., 2009; Tiede and Lang, 2010; De Paor and Whitmeyer, 2011; Blenkinsop, 2012; De Paor et al., 2012, 2016; Tavani et al., 2014Liang et al., 2018). Such developments have enhanced the shareability of 3D outcrop models aimed at the digital preservation of sites of special geological interest (i.e. geosites: Cayla, 2014; Burnham et al., 2022), the creation of virtual geological field trips (e.g. Eusden et al., 2012; Cliffe, 2017; Tavani et al., 2020a) and online digital outcrop model databases such as e-Rock (Cawood and Bond, 2019), V3Geo (Buckley et al., 2021), Svalbox (Senger et al., 2021), GeoTour3D, GeoBase, Virtual Australia, Sketchfab. The routine production of virtual outcrop models facilitated by ever-improving smartphones, offers a multitude of benefits in terms of science engagement and education, supporting virtual accessibility to globally significant outcrops that may be closed off to students and researchers (Bond and Cawood, 2021): a point which has been particularly relevant during the COVID-19 pandemic. Indeed, advantages associated with the integration of smartphones and tablets into the delivery of geoscience education have been recognized by numerous authors for more than a decade (e.g. Pavlis et al., 2010; Whitmeyer, 2012; Johnson and Johnston, 2013; Wallace and Witus, 2013; Lundmark et al., 2020; Senger and Nordmo, 2021). However, it is perhaps the urgent need for a replacement to physical fieldwork visits coupled with confluent developments in smartphone sensor technology and egalitarian 3D remote sensing data generation/sharing systems that are further elevating the role of smartphones in the field.

3. Testing the iPhone 12 Pro in the field

3.1. Location service

The iPhone 12 Pro is equipped with a GNSS receiver and comes with built-in support for GPS, GLONASS, Galileo, QZSS and BeiDou satellites systems. The GNSS raw data is not directly accessible and the location information in the iPhone 12 Pro is provided by the Apple Core Location framework, which combines data provided by all the localization capabilities available on the device, including the Wi-Fi network, GNSS, and Bluetooth. In contrast to most mobile phones and tablets, in which the GNSS signal is continuously updated to achieve a progressively accurate location (with errors up to the order of a few tens of cm after many tens of minutes of recording; e.g. Uradziński and Bakuła, 2020), the iPhone 12 Pro uses a fast stabilization procedure, which is not settable by the user, and provides final location data within only a few tens of seconds or less (Fig. 2). Despite the iPhone's fast stabilization, inability to control the stabilization procedure may represent an unwanted limitation in many situations.

We tested the accuracy of location data provided by the iPhone 12 Pro at ten sites in the Apennines of central Italy (Fig. 3A,B). All the sites are located within open countryside, far away from WI-FI routers, being representative of conditions commonly encountered during geological fieldwork. To record GNSS sensor data, we used the myTracks app, disabling the location service of the phone during the time interval between different acquisitions. Data collection was performed after placing the phone on the ground and recording 70-s tracks (counting after the activation of the location service) with a sampling rate of one recording per second. At each site, two tracks were recorded, one with network connections (i.e. mobile and Wi-Fi networks) enabled and one in airplane mode. During data acquisition, any interaction with the operator and electromagnetic energy emitting devices was avoided. At

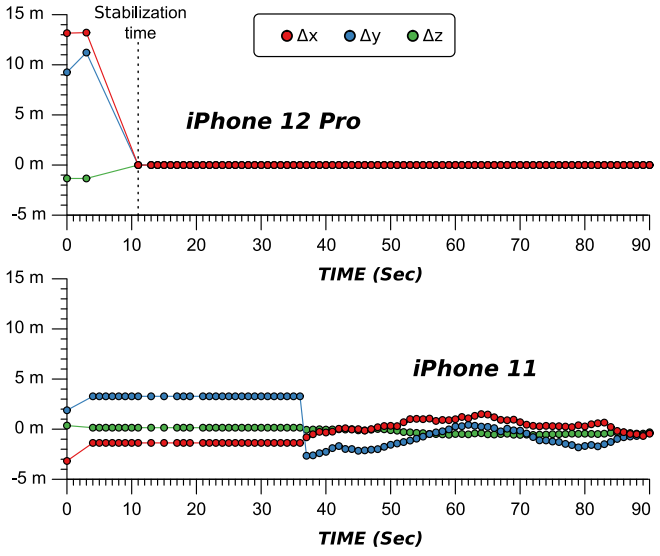

Fig. 2. Example of two (coeval) GNSS 90-s tracks recorded by the iPhone 12 Pro and the iPhone 11. For both tracks and for the three components (i.e. X, Y, and Z) the zero coincides with the last recorded value.

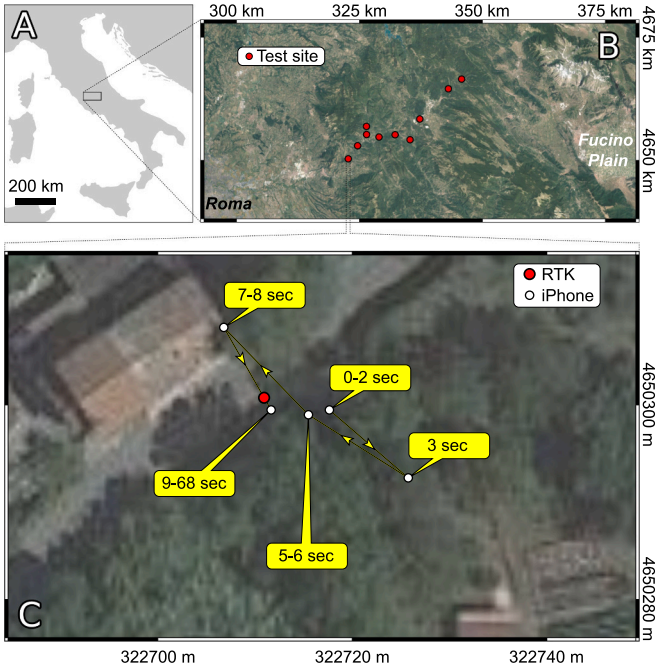

Fig. 3. GNSS test sites. (A,B) Location of the 10 sites in central Italy. (C) Example of an iPhone track, with ground truth data acquired using a Stonex S900 GNSS receiver (L1, L2 and L5) in Real-Time Kinematics (RTK) mode.

each site, ground truth data location of the smartphone was acquired using the latest-generation Stonex S900 GNSS receiver in Real-Time Kinematic (RTK) mode, with a base station belonging to the SmartNet network located a few kilometers away. At each site, the iPhone GNSS drift (i.e. the difference between the device's true location and the location recorded by the myTracks App) was calculated. In Fig. 3C, we show, in map view, the track recorded by the iPhone 12 Pro for Site 1. The track for the iPhone 12 Pro typically exhibits an initial period in which the native GNSS position deviates, followed by stabilization after ~9 s (Fig. 2).

Results from the GNSS analysis are shown in Fig. 4. For all ten sites, the value of the three drift components computed after stabilization, both in connected and airplane modes, is generally <10 m and the average error for each component is ~2 m (Fig. 4A). In our analysis, the stabilization time in Airplane mode (5.3 s on average; Fig. 4B) is smaller than in the connected mode (17 s on average; Fig. 4C); however, we noticed that this benchmark is not solely correlated to the acquisition mode, but rather was heavily dependent upon which of the two modes was performed first (i.e. first and second acquisition in Fig. 4B). Indeed, for eight out of ten sites, the track was firstly recorded in connected mode and then in airplane mode (exceptions are Sites 1 and 9). The average stabilization time for the second acquisition independently of the mode was indeed 4.6 s, which is lower than the average value for the airplane mode (Fig. 4B). Finally, it is worth noting that the accuracy of the measurement does not depend on the time needed by the phone to stabilize the signal (Fig. 4C).

3.2. *Digital compass*

From 2009 onwards, most mobile phones have been equipped with accelerometer and magnetometer sensors (Fig. 1A), with gyroscopes being introduced as standard sensors from 2010 onwards. These sensors (especially the magnetometer and gyroscope) are able to provide the orientation of the smartphone with respect to the magnetic north and to the vertical axis formed perpendicular to the Earth's surface. Consequently, geological applications requiring structural orientation

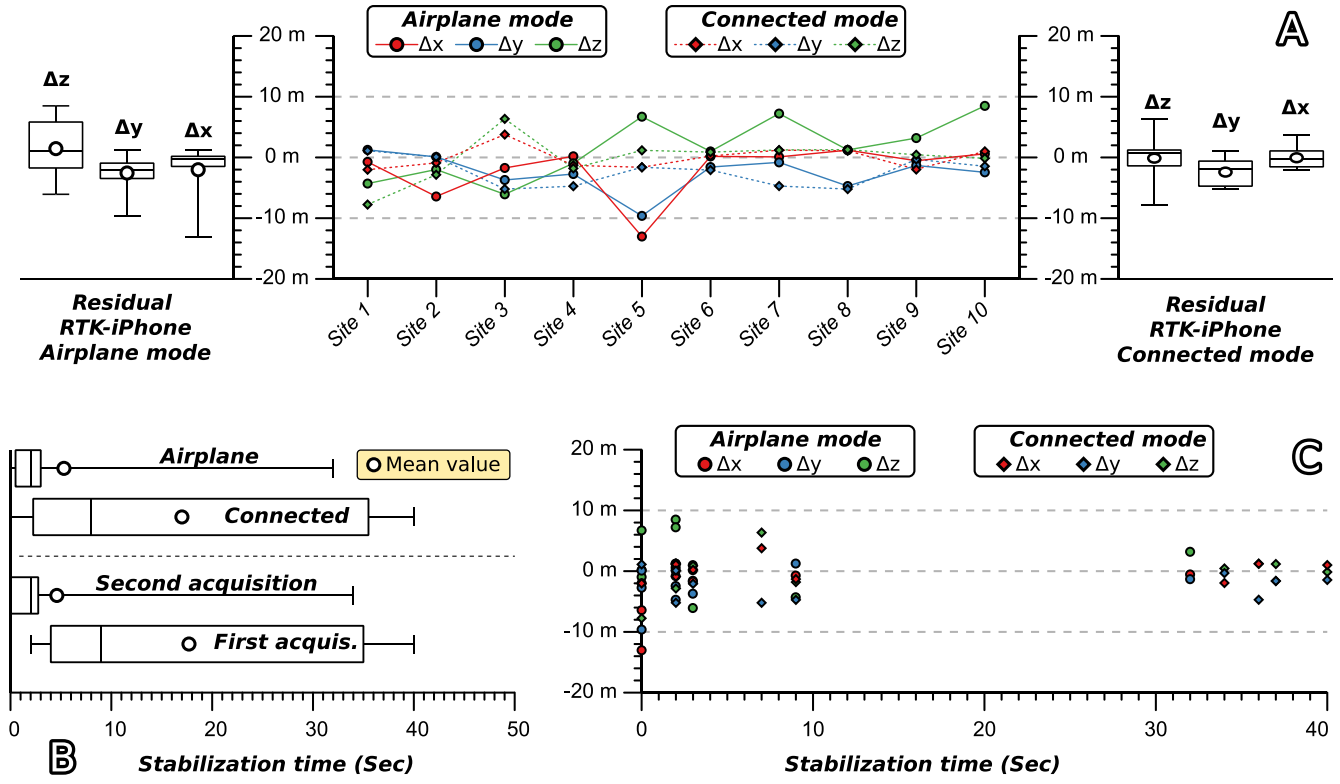

Fig. 4. Results of the GNSS test. (A) Difference between iPhone 12 Pro measurement and ground truth data in the ten sites for both airplane and connected modes, with box plots constructed using values of the tens sites. (B) Boxplots showing stabilization time. (C) Stabilization time vs difference between iPhone 12 Pro measurement and ground truth data.

measurements using smartphone inertial measurement unit (IMU) and magnetometer sensors have been developed (e.g. McCarthy et al., 2009; Weng et al., 2012; Allmendinger et al., 2017) (Fig. 1A). Accuracy tests carried out on a number of devices (e.g. Cawood et al., 2017; Novakova and Pavlis, 2019; Allmendinger et al., 2017) demonstrate the occurrence of strong variability in the precision of structural attitude measurements using different smartphones, with iOS devices generally performing better than Android devices in terms of accuracy.

We have carried out a test to reproduce operational conditions during fieldwork. Our test consists of 497 measurements of near-planar surfaces taken in the Apennines (Italy) during a four-month period (Fig. 5A). All the acquisition sites are located outdoors with the exception of one location, which is indoors and proximal to electrical sources. A 130 × 210 mm notebook with a rigid cover was employed to provide a stable platform upon the measured surfaces. Two measurements were taken for each surface: one using the iPhone 12 Pro and another using a Brunton Truarc 20 analog compass. In contrast to previous experiences with other smartphone devices, the iPhone 12 Pro did not require recalibration over the entirety of the acquisition period (5th March to 18th June 2021).

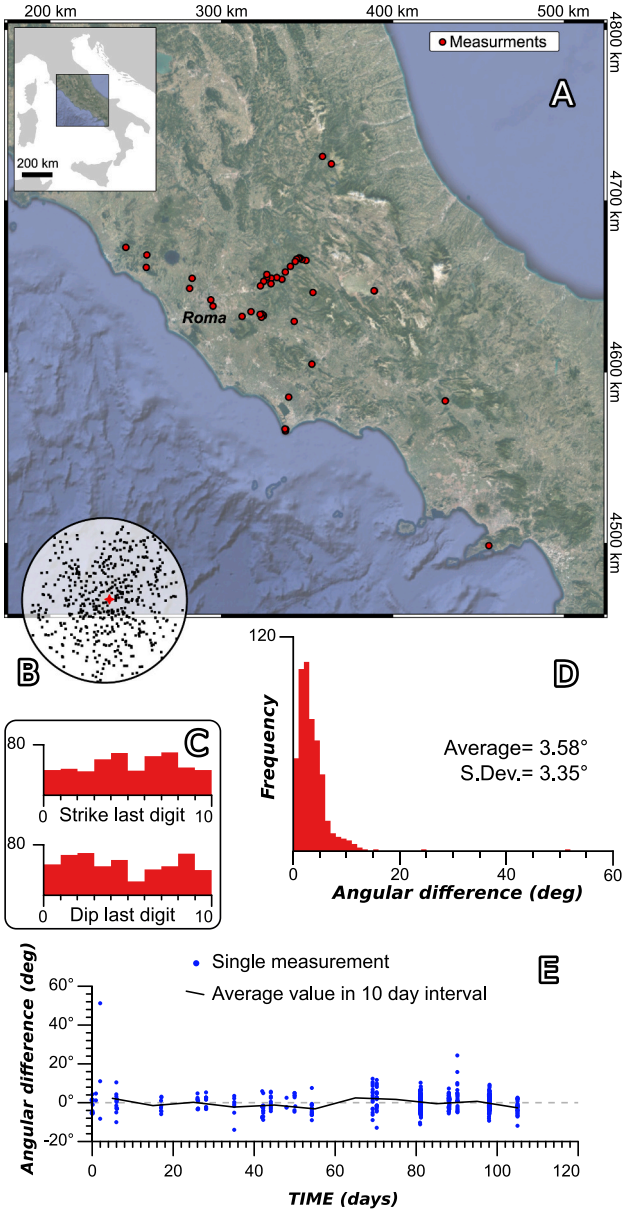

Fig. 5. *E*-compass test. (A) Location of measurements in central Italy. (B) Stereoplot of poles to measured planes, with the red star showing the average plane (mean plane by FieldClino). (C) Frequency distribution of the last digit of measurements taken with the analog compass (for both strike and dip components). (D) Frequency distribution of the angular difference between measurements taken with the analog compass and the iPhone 12 Pro, i.e. measurement error. (E) Distribution of error with time (time is set to zero at the first measurement. (For interpretation of the references to color in this figure legend, the reader is referred to the web version of this article.)

FieldMove Clino was used to acquire orientation measurements, which were only acquired after stabilization of the displayed value. Stabilization time typically depends on a combination of hardware and software (Allmendinger et al., 2017), and in the case of the iPhone is typically achieved within a couple of seconds. FieldMove Clino app stores data pre-corrected for magnetic declination. Accordingly, during the data processing, the declination was reintroduced for comparison with measurements taken using the analog compass-clinometer. The measured quasi-planar surfaces were randomly selected, as shown in the stereoplot of poles to planes (Fig. 5B). For parsimony, measurement error in the reading of the analog compass was neglected. For this reason, extra care was paid during measurements with the analog compass and approximation was avoided, as demonstrated by the frequency distribution of the last digit for both strike and dip measurements (Fig. 5C), with measurements taken with the accuracy of one degree. The difference between values provided by the iPhone (with no approximation) and by the analog compass is computed as the angular difference between the poles of the planes. The distribution of this difference (i.e. the error) is illustrated in Fig. 5D. The average error is 3.6° and the standard deviation is 3.4° and only 3.2% of measurements have an error exceeding 10°. One of these measurements is the only one that was tentatively taken indoors and has an error of ~50°. We have also evaluated the relationship between error and time elapsed since the phone unboxing (in our case the first measure has been taken two weeks after unboxing) and, as evidenced by results, the distribution of error has no relationship with this period (Fig. 5E). For each measurement, we have also computed the strike and dip difference between the digital (i.e. iPhone) and analog compass, in order to assess the main sources of error. As already established by other authors (e.g. Allmendinger et al., 2017), we recognise that the main source of error for orientation data is the azimuthal (strike) component (Fig. 6). Indeed, the total angular error is poorly correlated with the dip component (Fig. 6A), being essentially controlled by strike (Fig. 6B). It is worth noting that in Fig. 6A there are no points above the line with a slope of 45°, as the total angular difference is always greater than the dip difference.

Another major advantage of the iPhone 12 Pro over many Android devices is the stabilization time of the digital compass. Orientation measurements taken with Android phones typically require many seconds to stabilize, whereas measurements undertaken with the iPhone 12

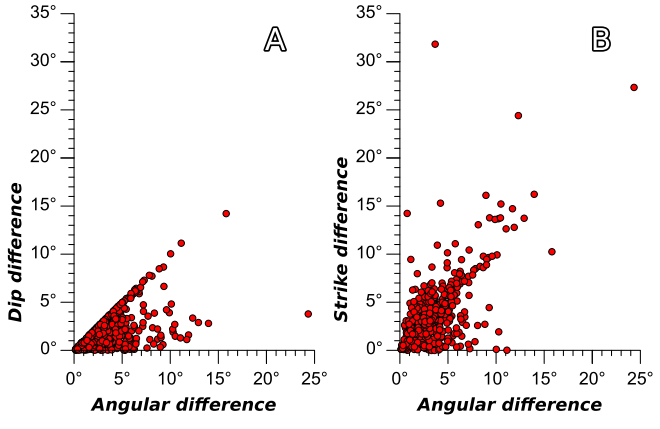

Fig. 6. Scatterplots of angular difference vs dip and strike components.

Pro are already stable after two seconds or less.

3.3. Optical and video-photographic properties

There are numerous detailed reviews by specialized websites testing the video-photographic capabilities of the iPhone 12 Pro. Such reviews are beyond the scope of this paper. Consequently, we will synthesize only the key results from the above-mentioned public domain reviews (dpreview.com; dxomark.com; techradar.com; tomsguide.com) to evaluate the device's capabilities for documenting field observations.

The iPhone 12 Pro is equipped with three rear cameras (12MP wide-angle, f/1.6; 12MP ultra-wide-angle, f/2.4; 12MP telephoto, f/2.0) with 2/2.5× optical and 10× digital zoom capacity, and a front camera (12MP TrueDepth, f/2.2). The lens of the main rear camera has dual optical image stabilization. The device, which is waterproof down to 6 m depth for 30 min (Rating IP68 according to the IEC 60529 standard), also houses a 6-core CPU with two performance cores and four efficient cores. At the time of our testing, this CPU outperformed all smartphone competitors for its computation (especially image processing) capacity. Moreover, the iPhone 12 Pro offers ProRAW functionality, combining the powerful RAW format with automatic post-production. The iPhone 12 Pro can shoot 4 K video using high dynamic range (Dolby Vision) and 60 fps.

We believe that, at present, there is no practical single digital replacement for the geological hand lens in the field. Despite this view, macrophotographic capabilities of smartphones offer interesting opportunities to document rock textures for further analysis, with geotags provided within each image's EXIF file providing spatial context to observations. To this end, the iPhone 12 Pro (like many other modern smartphones) is a powerful device for capturing macro photographs. In the iPhone 12 Pro, this type of photography is facilitated by the 2× optical zoom and 10× digital zoom, with dual-optical image stabilization on the wide and telephoto helping to mitigate motion blur. The iPhone 12 Pro Max also has a sensor-shift optical image stabilization feature for improved image capture quality. Macro-photography on the iPhone 12 Pro can also be aided by numerous user-friendly third-party lenses mounted on the existing lenses. As an example, we have taken photos of a 1 mm-sized fossil exposed on a polished rock surface using both the optical zoom of the iPhone and a third-party 24× lens (Fig. 7A). Photographs were taken with the iPhone using only the 2× optical zoom (shot at the minimum focal distance) (Fig. 7B), the 1× optical zoom plus the 24× additional lens (Fig. 7C), and the 2× optical zoom plus the 24× additional lens (Fig. 7D). Macroscopic details of the fossil are readily visible with images with the third party 24× lens, supporting the use of the iPhone in conjunction with an external macro lens as a viable replacement for or supplement to a classic hand lens.

3.4. Light detection and ranging (LiDAR)

LiDAR (Light Detection And Ranging), is a remote sensing technique based on laser light to measure range from the sensor to the scene. The iPhone/iPad LiDAR is based on the simultaneous emission of 576 beams and the maximum operational range is <5 m under optimal conditions (especially high albedo surfaces) (Luetzenburg et al., 2021). Our experience with this scanner in the field, however, indicates that the maximum range does not exceed ~3 m. Available scanning apps for iPhone employing LiDAR can be grouped into two types: (1) standalone LiDAR-based apps, such as 3D Scanner App or Polycam and (2) hybrid photogrammetry-LiDAR apps, including Pix4Dcatch and EveryPoint.

Among standalone LiDAR-based apps, we have tested the 3D Scanner App. It has a user-friendly interface, fast guided acquisition, relatively fast processing enabling results to be viewed directly in the field, good texture mapping capabilities, and generally accurate scaling of models. The app allows the user to directly measure distances on the screen with a claimed accuracy of ~1 cm. We have tested the accuracy of this measurement tool, and the accuracy of model scaling using a folding

Fig. 7. Example of results obtained with the use of additional analog microlens. (A) Microlens and photographed rock sample. (B) Photos taken with the built-in camera of the iPhone 12 Pro and with the additional microlens. The width of the images corresponds to the width of the phone's screen.

ruler within the scene (Fig. 8A). In detail, to test the model scaling accuracy, we generated 14 independent models of the ruler, each captured with progressive extension. We started by measuring the distance of 20 cm in the first model and progressed with increments of 10 cm. Differences between real and digital distances are in the order of 1 cm (Fig. 8B), in line with previous tests (Luetzenburg et al., 2021) and with

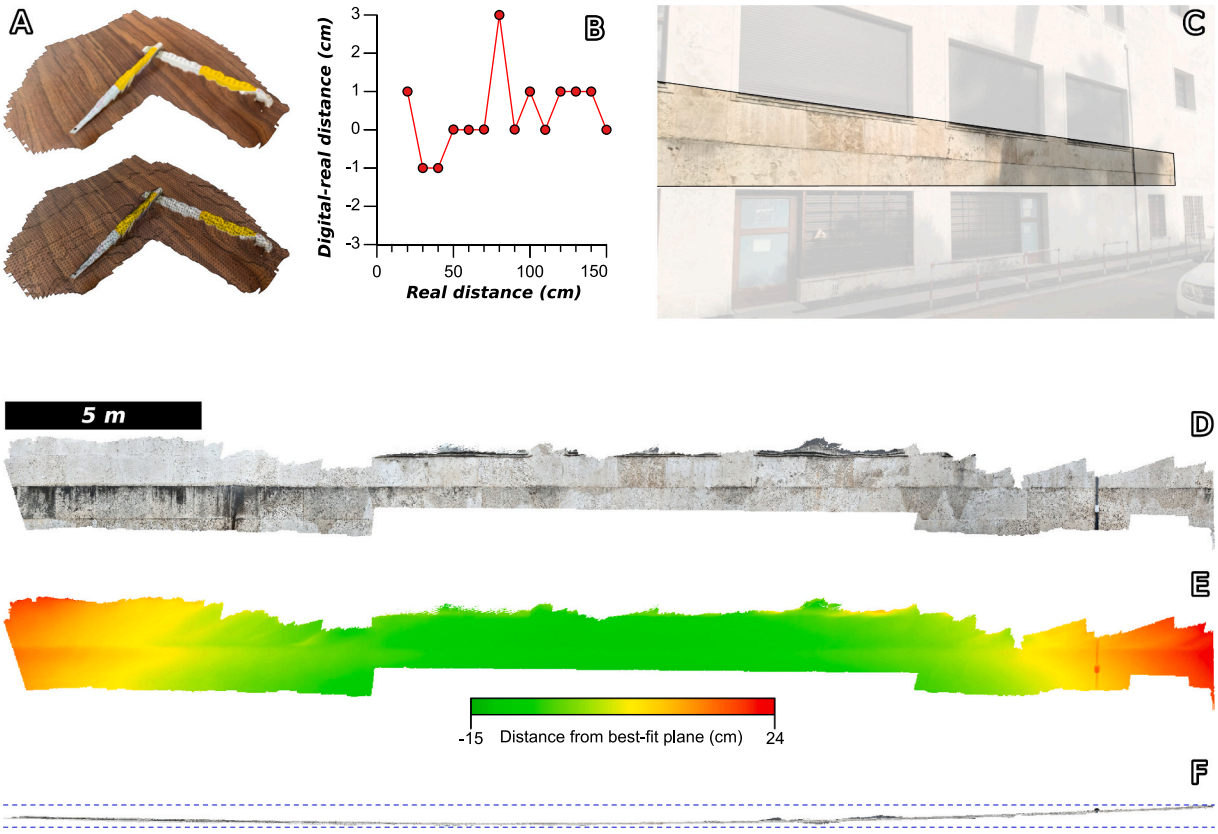

Fig. 8. LiDAR scanner test. (A) 3D digital model of the folding ruler used to test the accuracy of measurements taken with the 3D Scanner App. (B) Real distance vs difference between real and digital distances for the 14 models of the folding ruler. (C) External wall of the Dipartimento di Scienze della Terra of the Sapienza University, with the strip scanned with the 3D Scanner app indicated. (D) Frontal view of the digital model of the scanned strip. (E) Frontal view of the digital model, with color code indicating the distance from the best fit plane. (F) View from above of the scanned strip, evidencing the doming effect.

the declared accuracy of the app developer. In addition to the limited operational range (i.e. < 3 m), other limitations in the use of the iPhone Pro's LiDAR as a standalone scanner include: (i) the limited resolution of the output models (nominally 5–20 mm vertex spacings); (ii) the low resolution of the texture map due to limitations in the required processing time (required to avoid rapid battery discharge in the field); (iii) the lack of georeferencing support: the output model's Z axis aligns with that of the world frame, whereas model's azimuthal orientation is randomly determined (i.e. it is not intrinsically aligned with magnetic north); (iv) model deformations (doming), resulting from simultaneous localization and mapping (SLAM) errors, which are exacerbated when the user has to capture large scenes (i.e. > 10 m in width). This issue emanates from the phone pose estimation: when the user moves while scanning, the position of the phone relative to the previously scanned portion of the scene (the pose information) must be continuously re-determined to append the newly scanned portion of the scene to the model. This is achieved by merging the pose information as provided by visual and inertial sensors (Kelly and Sukhatme, 2011). Small errors in the phone's pose estimation can propagate errors in the surface reconstruction geometry for wide scenes and give rise to large-scale deformations in the reconstructed scene. These SLAM errors are roughly analogous to the so called 'doming effect', which can impact structure from motion - multiview stereo photogrammetric reconstructions (e.g. James and Robson, 2014; Magri and Toldo, 2017; Tavani et al., 2020). An example of this issue is illustrated in Fig. 8c-e, where scanning a 30 m wide vertical wall returns a deformed structure in the reconstruction.

A further application for the iPhone's LiDAR sensor is to produce digital models in conjunction with structure from motion - multiview stereo (SfM-MVS) photogrammetric reconstruction techniques. SfM-MVS models typically need post acquisition registration, which aims to properly orient, scale, and locate the reconstructed scene with respect to a local or global coordinate frame. The orientation of the iPhone, as provided by the Apple ARKit framework, the distance between phone and target objects as provided by LiDAR, and the location information provided by the GNSS sensor permit the georeferencing of SfM-MVS models built by using images captured using the iPhone 12 Pro. At present, this procedure is possible via the Pix4Dcatch (requiring a monthly subscription) and the EveryPoint (which includes a free version) apps for iPhone 12 Pro, both registering the camera pose information, thus providing the means for model georeferencing without the need for ground control points. For both apps, photo acquisition is done via the iPhone 12 Pro; for the Pix4Dcatch app, image processing is undertaken through a dedicated cloud service (Pix4Dcloud), whereas the EveryPoint app uses the iPhone's CPU and RAM. Tens of minutes to hours are typically needed to process data via the Pix4Dcloud cloud service, which, however, allows building dense point clouds, comparable with those produced via survey-grade laser-scanning. This, coupled with the need of uploading several MB of data, may restrict the ability to carry these steps out in the field. Conversely, whilst producing a less dense point cloud, scanning with EveryPoint returns results in near real time. Visual interpretation of models produced with EveryPoint reveals that, similarly to the 3D Scanner App, the vertical axis is properly set, whereas the Y and X axes of models have no relationship with magnetic north. In Fig. 9, two models of the same room are presented, produced using two independent acquisitions. Both models return vertical walls, as expected, but the same walls in the two models are not parallel. It appears that the Y axis of the model is essentially set parallel to the view direction of the first photo, indicating that a coarse local registration of the model may be achieved by ensuring that the optical axis of the first photo aligns with magnetic north. We have also tested the Pix4Dcatch

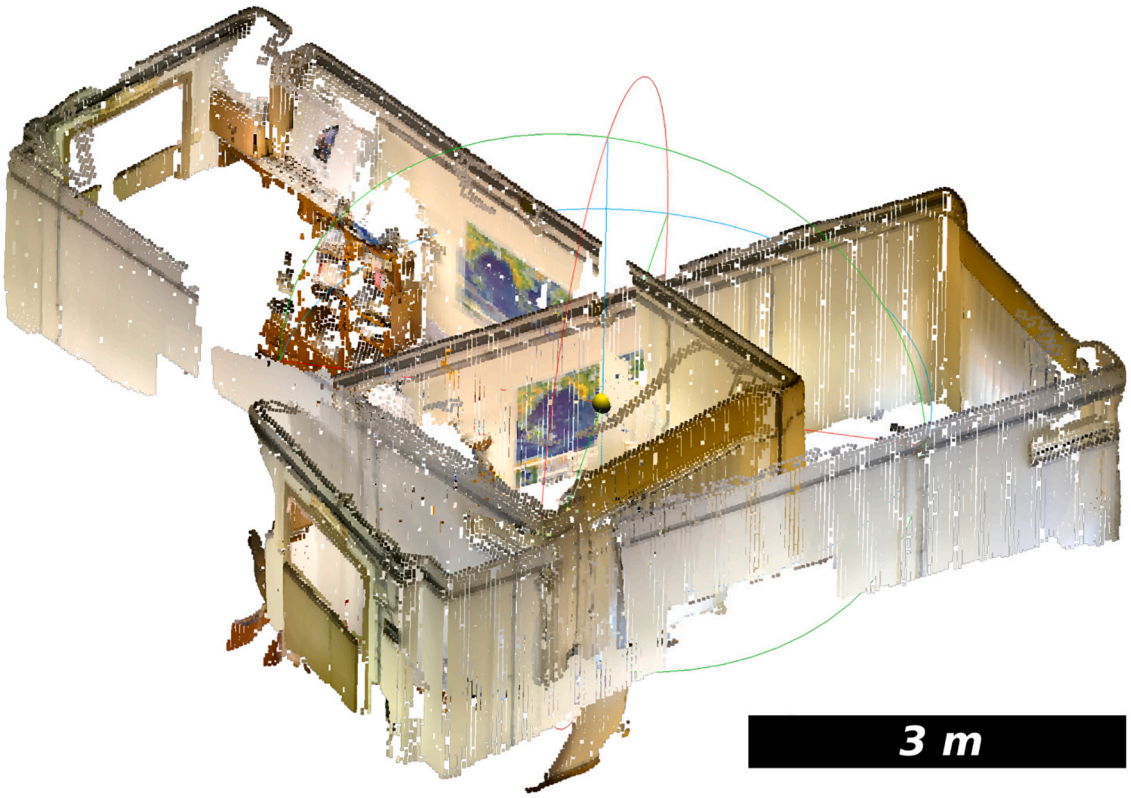

Fig. 9. Comparison between two 3D models of the same room of the Geodynamic lab at the Dipartimento di Scienze della Terra of the Sapienza University, obtained using the 3D Scanner App. The Z axis of the two models coincides and it is properly set (i.e. it coincides with the real world up axis), whereas the X and Y axes are rotated between the two models, and their orientation depends on the orientation of the phone when the acquisition starts.

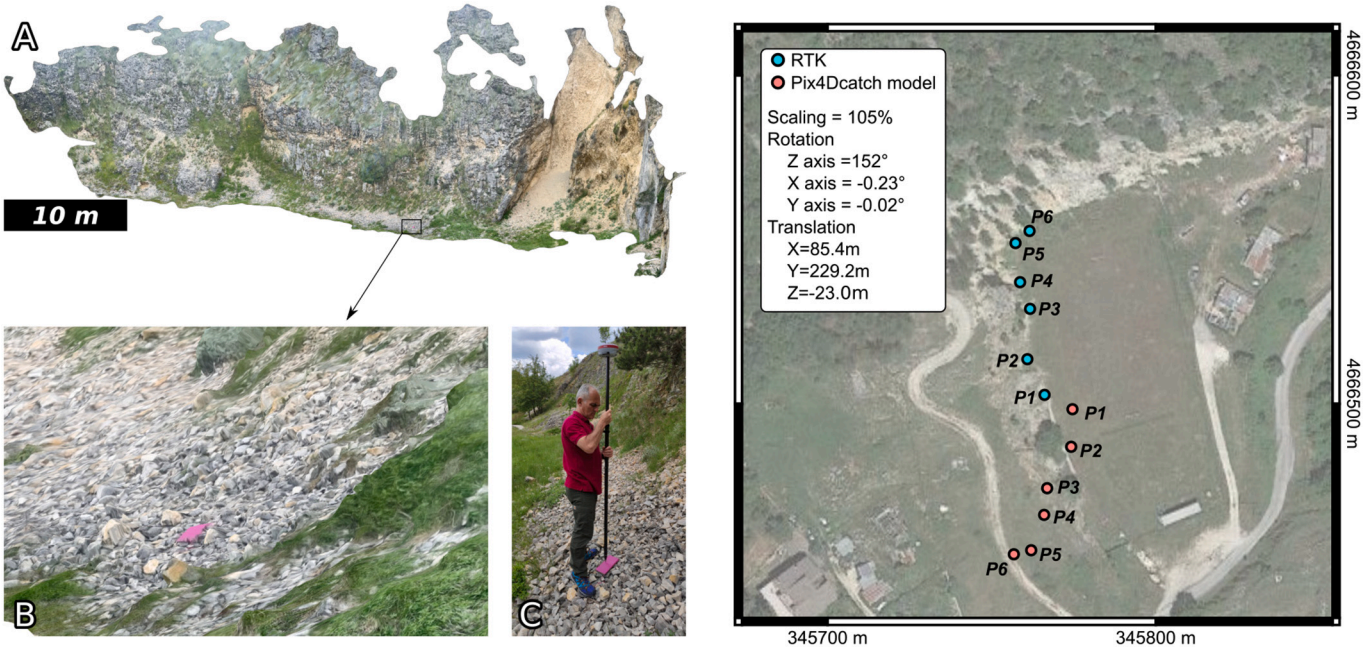

Fig. 10. (A) Digital outcrop of the hanging wall of the Pietrasecca fault (central Italy) acquired the Pix4Dscan App. Scanning has been carried out at a distance <5 m from the rock cliff and various key objects have been positioned in the model. (B) Example of a key object as seen in the digital model. (C) Measurement of the true position of the same object as in (b) independently carried out in the field with an RTK GNSS antenna. (D) Comparison of the position of key objects as determined in the model and as measured with the RTK antenna.

for iPhone 12 Pro app and, similarly to 3DScan and EveryPoint apps, models produced via Pix4Dcatch are properly oriented with respect to the world frame vertical axis but have arbitrary azimuthal orientations (relying on the Apple ARKit framework). Motivated by the high resolution of the generated models, we have extensively tested results from Pix4Dcatch. For example, in Fig. 10A, we present the reconstruction of a geological exposure close to the village of Pietrasecca in central Italy. The model was built during April 2021 and its orientation and scaling have not been modified. The location of six points in the digital model are compared with their actual location, as determined by a Stonex S900 GNSS receiver (L1, L2 and L5) in Real Time Kinematic (RTK) mode (Fig. 10b-d). To quantify the discrepancies, we have used the alignment tool of CloudCompare, where we have coupled homologous points in the virtual and real world. In order to let the model's measurements coincide with the RTK measurements, the following transformation must be applied: scaling = 105%; rotation about vertical axis = 152°; rotation about X axis = −0.23°; rotation about Y axis = −0.02°; ΔX = 85.4; ΔY = 229.2; ΔZ = −23.0 (original data are provided in the supplementary material). The high translation error is, by in large, related to the angular deviation between the RTK ground control points and their matched locations on the photogrammetric reconstruction. Very low angular deviations around the X and Y axes are in line with the other apps, confirming the capacity of the ARKit framework to recognise the world frame's vertical axis (i.e. using the phone's built in gyroscope sensor). Given that LiDAR data is associated with real-world scaling, it is somewhat surprising that the models have a relatively high scaling error (~5%), calling into question the benefits of mobile LiDAR augmented SfM-MVS for digital field data capture.

4. Discussion

Our tests carried out using the native LiDAR, digital compass and GNSS receiver of the iPhone 12 Pro were aimed at evaluating the usefulness of the device under typical fieldwork conditions. We have also reviewed the video/photo capabilities of the phone, including its capacity in replacing the magnifying lens for rock sample observation. It should be noted that, at the end of 2021, the iPhone 13 Pro was launched. This device houses an ostensibly similar array of sensors as the iPhone 12 Pro. We have also tested this newer device and our results are largely applicable to the updated system.

4.1. Location service

The iPhone 12 Pro is equipped with a GNSS receiver and supports all the major satellite systems. Some dual-frequency receivers on Android devices, with post-processing carrier phase fix, allows smartphone geolocation with accuracies of a few tens of cm under optimal conditions (e.g. Uradziński and Bakuła, 2020). However, in the case of the iPhone, raw geolocation data is not directly accessible, and the location is provided by the Apple Core Location framework, integrating satellite, wi-fi and telecommunication network resources, allowing stabilization of the estimated location after a few seconds or tens of seconds. Stabilization time reduces when the phone has already picked the position during a previous acquisition. This behavior has been confirmed during fieldwork carried out independently from this study, with the stabilization time reducing when the location service is active. The stabilization introduced in the iPhone 12 Pro is reached within a few seconds/tens of seconds. This, however, prevents the acquisition of GNSS raw data over longer periods; the acquisition of the GNSS raw data over periods in the order of tens of minutes is, indeed, a pre-requisite for GNSS post-processing carrier phase fix, required to achieve accuracies of a few tens of cm with dual frequency receivers. Consequently, reaching a location accuracy of tens of cm with the iPhone is prevented by both the hardware and the Apple Core Location framework, representing a major limitation of the device. On the other hand, having accuracies in the order of a few meters within seconds (see Fig. 4) is a major advantage when compared to other mobile devices, which may require minutes to gain an equivalent level of accuracy. Such fast stabilization characteristics could represent a strong improvement in some terrestrial SfM-MVS photogrammetry reconstruction, where models generated using mobile phone geotagged photos typically involve tens to hundreds of photos, for which decimating the stabilization time of the location results in a crucial improvement (Tavani et al., 2020b). On the other hand, for the same purpose, it could be useful to capture a few distal images (for a stable similarity transform needed to register the model) from a phone with a long GNSS stabilization period, so to achieve decimeter accuracy and use these for the final model registration. We acknowledge the availability of an RTK rover antenna that can be mounted onto the Apple iPhone 12 like a common cover. The rover geotags images with RTK accuracy, allowing one to build models with cm level accuracy. Though this add-on offers the extreme portability, the cost (more than three times that of the iPhone) prevents its use to the vast majority of users.

4.2. Compass

Our test includes ~500 measurements of planar features acquired in different locations over a period of four months without recalibration of the device. The average difference between the digital and analog measurements is ~3.6°, with a standard deviation of ~3.4°, in agreement with previous studies (e.g. Cawood et al., 2017; Allmendinger et al., 2017; Petroleum expert, 2021). It is worth remarking, however, that we had to assume that measurements made with the analog compass were error-free, which is of course a major simplification. Accordingly, we conclude that error when measuring with the iPhone 12 Pro is likely less than <3°. The main source of error in our analysis is related to the strike/trend, thus to the data provided by the magnetometer.

4.3. Video-photo

In general, the optical properties and the video-photographic capacity of mid- to high-end mobile phones are already comparable to reflex or mirrorless cameras, whilst being far less cumbersome. Due to this, the number of produced digital cameras has seen a steep decline since 2010 (https://www.statista.com/statistics/264336/world-production-of-digital-cameras-since-1999). The iPhone 12 Pro is considered at the forefront of all smartphones (dpreview.com; dxomark.com; techradar.com; tomsguide.com), making it an optimal tool for geological field surveys, which require video-photographic documentation. Though the video-photographic capabilities of the iPhone 12 Pro are excellent (at least for a smartphone), we acknowledge that camera specifications have been improved in the iPhone 12 Pro Max and, more recently, in the iPhone 13 Pro (apple.com; dpreview.com). Among other important features, the size of photographic sensors and related pixels has been expanded, optical and digital zooms have been strengthened, macro photograph mode has been implemented, the CPU has been updated, the battery has been made longer-lasting, and stabilization has been added directly to the sensors. It is worth mentioning here that the new LiDAR-equipped iPhone 13 Pro has been recently awarded for the best smartphone camera in 2021 by the prestigious online magazine DPReview.

The possibility of adding external macro lenses, makes the iPhone, as well as equivalently equipped smartphones, suitable for inspection of fossils and micro-structures directly in the field, with the advantages over the analog lens that digital microphotos can be stored, geotagged, and annotated, as well as shared in real time. Lastly, the notably high quality of geotagged and oriented photographs produced by the iPhone 12 Pro makes this mobile device particularly useful for the acquisition of images that can be later implemented in SfM-MVS software for the production of fully georeferenced models of geological exposures (e.g. Tavani et al., 2020b; Corradetti et al., 2021b).

4.4. Lidar

Here, we have to somewhat dampen the enthusiasm for the iPhone LiDAR as a medium for digital outcrop data capture and analysis. It is important to note that the specifications and performances of the iPhone/iPad LiDAR sensor are by far not equivalent to survey-grade LiDAR tools in terms of resolution (i.e. points per square meter), maximum operational range (presently <5 m) or noise characteristics. These iPhone LiDAR's output scans are closer in terms of these key characteristics to those output scans by structured light cameras, which are already available for mobile devices (e.g. the Occidental Structure Sensor), albeit being by far less user friendly than the iPhone's native LiDAR.

Present challenges in obtaining a fully georeferenced model using the iPhone's LiDAR, ostensibly due to its integration with the Apple ARkit framework, represents another major limitation for applications beyond visualization. An easy solution for this problem is to measure the orientation of reference objects or natural near planar discontinuities (such as fractures or bedding surfaces) within the scene, to later properly reorient the model (e.g. Fleming and Pavlis, 2018; Wang et al., 2021). Nevertheless, the iPhone LiDAR represents an excellent, highly portable tool for rapid documentation of 3D outcrop geometry and texture, opening the door to sharing geological exposures for the purpose of educational and outreach activities. Rapid and easy acquisition via free apps, such as 3D Scaner App, permits uploading relatively light virtual outcrop models in public repositories, such as sketchfab (https://sketchfab.com), with full accessibility for the general public. We hope that the streamlined virtual outcrop model generation and sharing facilitated by the iPhone LiDAR will bring this tactile visualization medium to a much broader user base of educators, and students.

4.5. Smartphone assisted fieldwork: present and future

The results obtained by this study are to be considered as positive concerning the iPhone 12 Pro's compass, geolocation and video-photo capabilities, with respect to their utility for general geological fieldwork. In addition, the LiDAR sensor represents a useful tool for documenting exposures compared to classical outcrop photography. The quite good scaling accuracy of the models also allows for certain virtual outcrop-based metrics to be ascertained directly in the field, e.g. measurement of true bed thicknesses using the measurement tool of the tested 3D scanning apps. The greatest weakness of smartphones, in the frame of fieldwork, is the replacement of mapping and annotation tools. Although several apps are available for creating various kinds of notes that adapt well to the needs of geological fieldwork, the relatively small size of the screen makes smartphones an awkward annotation tool, useful only for basic operations, such as adding comments to geotagged images. Even more complicated is mapping with the iPhone, as the <7 in. size of the iPhone 12 Pro and Pro max screen makes it hard to read and edit maps. For mapping and creating geotagged notes and sketches, tablets are undoubtedly a preferable tool to smartphones (e.g. Senger and Nordmo, 2021). Although apps for geological surveying, such as FieldMove (Vaughan et al., 2014), Qfield (e.g. De Donatis et al., 2016), StraboSpot (Glazner and Walker, 2020), or KMapper (Yeon, 2021), generally provide both smartphone and tablet support, anecdotally, the majority of practitioners prefer the use of tablets for digital field mapping. The recent advent of foldable smartphones could provide a viable way to implement all the advantages of tablets within smartphones. In spite of the above, insufficient screen brightness on sunny days, battery duration issues when mapping in remote areas, and other logistical issues mean that an all-weather paper fieldbook should always form part of the geologist's field kit.

From a practical point of view the digital transition of fieldwork has already occurred. In most cases, paper fieldbooks, maps, analog or digital compasses, and handheld GNSS receivers are backup tools, often left in the geologist's backpack having been effectively replaced by sensors/apps within smartphones and tablets. Whilst the iPhone LiDAR provides a novel method of 3D scene capture compared to 2D photos, more established SfM-MVS photogrammetry, which is readily deployable from mobile devices equipped with cameras, remains a more viable option for digital outcrop data capture, particularly for large scenes.

Synchronized employment of smartphones for data collection and tablets for mapping and annotation is a mode of operation that has increased the geological data acquisition speed within the field, and negates the need for time-consuming digitization back in the office. The combined use of tablets and smartphones also ensures reciprocal backups at the end of each field day. Digital acquisition also improves consistency between data acquired by different users and imposes a common format for exchanging geological data. This practice, coupled with data sharing, will prevent the need for repeated access to the same outcrop from different users. Digitization and data sharing boosts collaboration between geographically disparate researchers while limiting geologists' travel requirements, thus reducing CO_2 emissions. The rise of open access databases for geological outcrop data sharing (e.g. Outcropedia, https://outcropedia.tectask.org/; eRock: https://www.e-rock.co.uk/) is likely to boost such collaborations. In the case of eRock, interactive 3D outcrop models are embedded into the website using sketchfab (https://sketchfab.com/), providing access to such data types to teachers/students without the need for high-end PCs (e.g. Fleming, 2022).

Smartphone assisted fieldwork and digital fieldwork in general have major advantages when preparing material for teaching and education, including the fact that smartphones may also serve as remote controllers for drones. The employment of smartphones and tablets for student training has many benefits (e.g. Pavlis et al., 2010; Whitmeyer, 2012; Johnson and Johnston, 2013; Wallace and Witus, 2013; Lundmark et al., 2020; Senger and Nordmo, 2021), perhaps the greatest of which is that they are ubiquitous tools, the basic operation of which is already familiar to the vast majority of the student cohort. Obtaining structural measurements with smartphones in place of analog compasses is faster and easier for students, and the possibility of viewing in real-time measurements on map or on stereoplots provides a more direct learning experience for many. The major limitation is that, according to both our direct experience and published works (e.g. Novakova and Pavlis, 2019), many Android devices are not sufficiently precise for taking reliable measurements. Nevertheless, having available a LiDAR (such as for the iPhone 12 Pro) for scanning outcrops in 3D could engage students in generating data and perhaps overall increases the understanding of the intrinsic 3D aspects of geological outcrops (this is an important avenue of educational research, at present still largely unexplored). This partly compensates for those limitations that are perhaps of greatest concerns to educators of geological mapping among other disciplines. One of these limitations concerns the difference between mapping and collecting data. Mapping, indeed, requires landscape reading and navigation, and the understanding of the collected data within its 3D geological framework. The instantaneous availability of each field observation via GNSS tags may slow down the development of 3D thinking: a prerequisite for the interpretation of panoramic views of a field location (to mitigate this issue, we generally provide students with both orthophotos and digital topographic maps). Another critical point is the possibility of annotating images and drawing onto them, which is a fantastic option for expert geologists, whilst should be used with caution by students, for which the exercise of schematizing an outcrop is a fundamental step in the learning process. In this case, we favor both pencil and paper and drawing tools in tablets.

In conclusion, acquiring geological data until now has typically been undertaken during planned campaigns, for which the geologist's backpack was prepared and filled with an array of tools. The recently released iPhone 12 Pro is able to replace almost all these tools (some outstandingly, others in a less optimal way), with its LiDAR scanner providing an additional way of documenting exposures that can be achieved even during casual observation of outcrops by both experts and

Fig. 11. Workflow for uploading 3D outcrop models in google maps. Scanning of outcrops with handheld devices can be done via iPhone/iPad LiDAR or smartphone/drone photogrammetry. Resulting models are uploaded in Sketchfab, where title, description, category and tags are defined, and where the scene setting is defined (i.e. initial view, orientation of the model). Points/views of interest can be also defined as annotations. In Google Maps, geological exposures can be uploaded by right-clicking the location of the outcrop and selecting "Add missing place". Enter the outcrop's title and in the description select "tourist attraction", and in the web link paste the URL of the sketchfab model. To add information or link to published papers or databases, we recommend using the section dedicated to comments. At this point, any user searching for "tourist attraction" nearby, will find the uploaded geological outcrop. Example sites can be found here:
https://goo.gl/maps/nAUBFGwEDLcDYywQA
https://goo.gl/maps/H7QsJrRvnGG9GpRw7

novices. Taking advantage of this unprecedented possibility presents major opportunities for public engagement within the geosciences. In this sense, independent of the scanning methods used (i.e. iPhone LiDAR or photogrammetry via smartphone or drone), the possibility of placing geological exposures (previously uploaded in public repositories such as sketchfab) into Google Maps (Fig. 11), by treating them as "tourist attraction" (a request for creating the "Geological outcrop" category has been submitted to Google) and making them available to professionals, officials, journalists or simply curious members of the public (see the following YouTube video: https://youtu.be/xRlSMvpzSSU) could represent a paradigm shift in the perception and dissemination of geosciences.

5. Conclusions

Smartphone assisted fieldwork defines a mode of carrying out fieldwork in which smartphones (possibly in conjunction with tablets for mapping and annotations) are the core platform for field measurements and activities, allowing geologists to accelerate data acquisition and favoring the emergence of common file formats and storage repositories for field data. Among current smartphones, the reviewed iPhone Pro has leading standards in terms of location accuracy, attitude measurements, photo/video capture, and it can replace equivalent analog and stand-alone tools. With its newly equipped LiDAR sensor, the iPhone Pro is capable of producing 3D surface reconstructions of outcrops suitable for geo-documentation, casual data sharing and visualization, though

limitations of presently available LiDAR capture and processing apps for the device create a technical bottleneck in terms of model registration. In essence, the iPhone Pro represents an incredibly versatile geological tool, allowing users to capture multimodal geological dataset from a single platform and instantly share them with a global community via popular geo-browsers such as Google Maps. In summary, with reference to the progress trajectory represented in Fig. 1, the iPhone makes the use of several digital tools and data for the inspection of geological landscapes user-friendly and accessible to a vast audience of both expert and practitioners. This significantly moves our state forward in the digital transition of geoscience fieldwork and will potentially involve in this work not only professional geologists or scientists, but also students, public officials, and curious citizens alike via the digital field.

Supplementary data to this article can be found online at https://doi.org/10.1016/j.earscirev.2022.103969.

Declaration of Competing Interest

Authors are reporting no potential conflict of interest.

Acknowledgements

ST acknowledges financial support from the Italian Ministry of University and Research (MIUR). AC acknowledges Microgrants 2021 resources, funded by the FVG Region (LR 2/2011 “Finanziamenti al Sistema Universitario regionale”). Funding by Sapienza Progetti di Avvio alla Ricerca 2020 to MM is acknowledged. Funding by Progetti di Ateneo Sapienza (2019) to Eugenio Carminati is acknowledged. Silvia Mittempergher and an anonymous reviewer, as well as the Editor Shuhab Khan, are thanked for their thoughtful and positive reviews that improved this paper.

References

Allmendinger, R.W., Siron, C.R., Scott, C.P., 2017. Structural data collection with mobile devices: accuracy, redundancy, and best practices. J. Struct. Geol. 102, 98–112. https://doi.org/10.1016/j.jsg.2017.07.011.

Anadu, J., Ali, H., Jackson, C., 2020. Ten steps to protect BIPOC scholars in the field. Eos 101. https://doi.org/10.1029/2020EO150525.

Arbués, P., García-Sellés, D., Granado, P., López-Blanco, M., Muñoz, J.A., 2012. A method for producing photorealistic digital outcrop models. In: 74th EAGE Conference and Exhibition incorporating EUROPEC 2012 (pp. cp-293). European Association of Geoscientists & Engineers. https://doi.org/10.3997/2214-4609.20148218.

Bates, K.T., Manning, P.L., Vila, B., Hodgetts, D., 2008. Three-dimensional modelling and analysis of dinosaur trackways. Palaeontology 51, 999–1010. https://doi.org/10.1111/j.1475-4983.2008.00789.x.

Bellian, J.A., Kerans, C., Jennette, D.C., 2005. Digital outcrop models: applications of terrestrial scanning lidar technology in stratigraphic modeling. J. Sediment. Res. 75 (2), 166–176. https://doi.org/10.2110/jsr.2005.013.

Bemis, S.P., Micklethwaite, S., Turner, D., James, M.R., Akciz, S., Thiele, S.T., Bangash, H.A., 2014. Ground-based and UAV-based photogrammetry: a multi-scale, high-resolution mapping tool for structural geology and paleoseismology. J. Struct. Geol. 69, 163–178. https://doi.org/10.1016/j.jsg.2014.10.007.

Bistacchi, A., Griffith, W.A., Smith, S.A., Di Toro, G., Jones, R., Nielsen, S., 2011. Fault roughness at seismogenic depths from LIDAR and photogrammetric analysis. Pure Appl. Geophys. 168 (12), 2345–2363. https://doi.org/10.1007/s00024-011-0301-7.

Blenkinsop, T.G., 2012. Visualizing structural geology: from excel to Google Earth. Comput. Geosci. 45, 52–56. https://doi.org/10.1016/j.cageo.2012.03.007.

Bond, C.E., Cawood, A.J., 2021. A role for virtual outcrop models in blended learning–improved 3D thinking and positive perceptions of learning. Geosci. Commun. 4 (2), 233–244. https://doi.org/10.5194/gc-4-233-2021.

Brimhall, G., 1998. Direct Digital Field Mapping Using Pen-Based PC Computers Supported by Differential Global Positioning Systems and Laser Range Finders: Geological Society of America Annual Meeting, Abstracts with Program v.30(7), p. A-256.

Brimhall, G.H., Vanegas, A., 2001. Removing science workflow barriers to adoption of digital geological mapping by using the GeoMapper universal program and visual user interface. In: Soller, D.R. (Ed.), Digital Mapping Techniques' 01-Workshop Proceedings: U.S. Geological Survey Open File Report 01–223, pp. 103–114.

Briner, A.P., Kronenberg, H., Mazurek, M., Horn, H., Engi, M., Peters, T., 1999. FieldBook and GeoDatabase: tools for field data acquisition and analysis. Comput. Geosci. 25, 1101–1111. https://doi.org/10.1016/S0098-3004(99)00078-3.

Brodaric, B., 1997. Field data capture and manipulation using GSC filed log v.3.0. In: Soller, D.R. (Ed.), Proceedings of a Workshop on Digital Mapping Techniques: Methods for Geologic Map Data Capture, Management, and Publication: U.S. Geological Survey, Open-file Report 97–269, pp. 77–81.

Brodu, N., Lague, D., 2012. 3D terrestrial lidar data classification of complex natural scenes using a multi-scale dimensionality criterion: applications in geomorphology. ISPRS J. Photogramm. Remote Sens. 68, 121–134. https://doi.org/10.1016/j.isprsjprs.2012.01.006.

Buckley, S.J., Howell, J.A., Naumann, N., Lewis, C., Chmielewska, M., Ringdal, K., Vanbiervliet, J., Tong, B., Mulelid-Tynes, O.S., Foster, D., et al., 2021. V3Geo: a cloud-based repository for virtual 3D models in geoscience. Geosci. Commun. Discuss. 1–27. https://doi.org/10.5194/gc-2021-30.

Burchfiel, B.C., 2004. New technology; New geological challenges. GSA Today 14, 4–10. https://doi.org/10.1130/1052-5173(2004)014<0004:NTNGC>2.0.CO;2.

Burnham, B.S., Bond, C., Flaig, P.P., van der Kolk, D.A., Hodgetts, D., 2022. Outcrop conservation: promoting accessibility, inclusivity, and reproducibility through digital preservation. Sediment. Rec. 20, 5–14. https://doi.org/10.2110/sedred.2022.1.2.

Bursztyn, N., Shelton, B., Walker, A., Pederson, J., 2017. Increasing undergraduate interest to learn geoscience with GPS-based augmented reality field trips on students' own smartphones. GSA Today 27, 4–10. https://doi.org/10.1130/GSATG304A.1.

Butler, D., 2006. Virtual globes: the web-wide world. Nature 439, 776–778. https://doi.org/10.1038/439776a.

Carbonell Carrera, C., Bermejo Asensio, L.A., 2017. Augmented reality as a digital teaching environment to develop spatial thinking. Cartogr. Geogr. Inf. Sc. 44, 259–270. https://doi.org/10.1080/15230406.2016.1145556.

Carver, S., Heywood, I., Cornelius, S., Sear, D., 1995. Evaluating field-based GIS for environmental characterization, modelling and decision support. Int. J. Geogr. Inf. Syst. 9 (4), 475–486. https://doi.org/10.1080/02693799508902051.

Cawood, A.J., Bond, C.E., 2019. eRock: an open-access repository of virtual outcrops for geoscience education. GSA Today 29, 36–37.

Cawood, A.J., Bond, C.E., Howell, J.A., Butler, R.W., Totake, Y., 2017. LiDAR, UAV or compass-clinometer? Accuracy, coverage and the effects on structural models. J. Struct. Geol. 98, 67–82. https://doi.org/10.1016/j.jsg.2017.04.004.

Cawood, A.J., Corradetti, A., Granado, P., Tavani, S., 2022. Detailed structural analysis of digital outcrops: a learning example from the Kermanshah-Qulqula radiolarite basin, Zagros Belt. Iran. J. Struct. Geol. 154, 104489. https://doi.org/10.1016/j.jsg.2021.104489.

Cayla, N., 2014. An overview of new technologies applied to the management of geoheritage. Geoheritage 6, 91–102. https://doi.org/10.1007/s12371-014-0113-0.

Chen, A., Leptoukh, G., Kempler, S., Lynnes, C., Savtchenko, A., Nadeau, D., Farley, J., 2009. Visualization of A-train vertical profiles using Google Earth. Comput. Geosci. 35, 419–427. https://doi.org/10.1016/j.cageo.2008.08.006.

Clegg, P., Bruciatelli, L., Domingos, F., Jones, R.R., De Donatis, M., Wilson, R.W., 2006. Digital geological mapping with tablet PC and PDA: a comparison. Comput. Geosci. 32 (10), 1682–1698. https://doi.org/10.1016/j.cageo.2006.03.007.

Cliffe, A.D., 2017. A review of the benefits and drawbacks to virtual field guides in today's Geoscience higher education environment. Int. J. Educ. Technol. High. Educ. 14, 1–14. https://doi.org/10.1186/s41239-017-0066-x.

Corradetti, A., Zambrano, M., Tavani, S., Tondi, E., Seers, T.D., 2021a. The impact of weathering upon the roughness characteristics of a splay of the active fault system responsible for the massive 2016 seismic sequence of the Central Apennines, Italy. Bulletin 133 (3–4), 885–896. https://doi.org/10.1130/B35661.1.

Corradetti, A., Seers, T.D., Billi, A., Tavani, S., 2021b. Virtual outcrops in a pocket: the smartphone as a fully equipped photogrammetric data acquisition tool. GSA Today 31, 4–9. https://doi.org/10.1130/GSATG506A.1.

De Donatis, M., Bruciatelli, L., 2006. MAP IT: the GIS software for field mapping with tablet pc. Comput. Geosci. 32, 673–680. https://doi.org/10.1016/j.cageo.2005.09.003.

De Donatis, M., Alberti, M., Cesarini, C., Menichetti, M., Susini, S., 2016. Open source GIS for geological field mapping: research and teaching experience. PeerJ Preprints 4 e2258v1.

De Paor, D., 2016. Virtual rocks. GSA Today 26, 4–11. https://doi.org/10.1130/GSATG257A.1.

De Paor, D.G., Whitmeyer, S.J., 2011. Geological and geophysical modeling on virtual globes using KML, COLLADA, and Javascript. Comput. Geosci. 37 (1), 100–110.

De Paor, D.G., Wild, S.C., Dordevic, M.M., 2012. Emergent and animated COLLADA models of the Tonga Trench and Samoa Archipelago: implications for geoscience modeling, education, and research. Geosphere 8, 491–506. https://doi.org/10.1130/GES00758.1.

De Paor, D.G., Dordevic, M.M., Karabinos, P., Tewksbury, B.J., Whitmeyer, S.J., 2016. The fold analysis challenge: a virtual globe-based educational resource. J. Struct. Geol. 85, 85–94. https://doi.org/10.1016/j.jsg.2016.02.005.

Eusden, J.D., Duvall, M., Bryant, M., 2012. Google Earth mashup of the geology in the Presidential Range, New Hampshire: linking real and virtual field trips for an introductory geology class. Geol. Soc. Am. Spec. Pap. 492, 355–366. https://doi.org/10.1130/2012.2492(26).

Favalli, M., Fornaciai, A., Mazzarini, F., Harris, A., Neri, M., Behncke, B., Pareschi, M.T., Tarquini, S., Boschi, E., 2010. Evolution of an active lava flow field using a multitemporal LIDAR acquisition. J. Geophys. Res. Solid Earth 115, B11203. https://doi.org/10.1029/2010JB007463.

Favalli, M., Fornaciai, A., Isola, I., Tarquini, S., Nannipieri, L., 2012. Multiview 3D reconstruction in geosciences. Comput. Geosci. 44, 168–176. https://doi.org/10.1016/j.cageo.2011.09.012.

Fernández, O., Muñoz, J.A., Arbués, P., Falivene, O., Marzo, M., 2004. Three-dimensional reconstruction of geological surfaces: an example of growth strata and

turbidite systems from the Ainsa basin (Pyrenees, Spain). AAPG Bull. 88 (8), 1049–1068. https://doi.org/10.1306/02260403062.
Fleming, Z., 2022. Using virtual outcrop models and Google Earth to teach structural geology concepts. J. Struct. Geol. https://doi.org/10.1016/j.jsg.2022.104537. Under Review.
Fleming, Z., Pavlis, T., 2018. An orientation based correction method for SfM-MVS point clouds—Implications for field geology. J. Struct. Geol. 113, 76–89. https://doi.org/10.1016/j.jsg.2018.05.014.
Franceschi, M., Teza, G., Preto, N., Pesci, A., Galgaro, A., Girardi, S., 2009. Discrimination between marls and limestones using intensity data from terrestrial laser scanner. ISPRS J. Photogramm. Remote Sens. 64, 522–528. https://doi.org/10.1016/j.isprsjprs.2009.03.003.
Furukawa, Y., 2010. PMVS2. https://grail.cs.washington.edu/software/pmvs/.
García-Sellés, D., Falivene, O., Arbués, P., Gratacos, O., Tavani, S., Munoz, J.A., 2011. Supervised identification and reconstruction of near-planar geological surfaces from terrestrial laser scanning. Comput. Geosci. 37 (10), 1584–1594. https://doi.org/10.1016/j.cageo.2011.03.007.
Glazner, A.F., Walker, J.D., 2020. StraboTools: a mobile app for quantifying rock fabric. GSA Today 30, 4–10. https://doi.org/10.1130/GSATG454A.1.
Hartzell, P., Glennie, C., Biber, K., Khan, S., 2014. Application of multispectral LiDAR to automated virtual outcrop geology. ISPRS J. Photogramm. Remote Sens. 88, 147–155. https://doi.org/10.1016/j.isprsjprs.2013.12.004.
Hudnut, K.W., Borsa, A., Glennie, C., Minster, J.B., 2002. High-resolution topography along surface rupture of the 16 October 1999 Hector Mine, California, earthquake (M w 7.1) from airborne laser swath mapping. Bull. Seismol. Soc. Am. 92, 1570–1576. https://doi.org/10.1785/0120000934.
James, M.R., Robson, S., 2012. Straightforward reconstruction of 3D surfaces and topography with a camera: accuracy and geoscience application. J. Geophys. Res. Earth Surf. 117, F03017. https://doi.org/10.1029/2011JF002289.
James, M.R., Robson, S., 2014. Mitigating systematic error in topographic models derived from UAV and ground-based image networks. Earth Surf. Process. Landf. 39, 1413–1420. https://doi.org/10.1002/esp.3609.
Johnson, Z.I., Johnston, D.W., 2013. Smartphones: powerful tools for geoscience education. EOS Trans. Am. Geophys. Union 94 (47), 433–434. https://doi.org/10.1002/2013EO470001.
Jones, R.R., McCaffrey, K.J., Wilson, R.W., Holdsworth, R.E., 2004. Digital field data acquisition: towards increased quantification of uncertainty during geological mapping. Geol. Soc. Lond., Spec. Publ. 239 (1), 43–56. https://doi.org/10.1144/GSL.SP.2004.239.01.04.
Kelly, J., Sukhatme, G.S., 2011. Visual-inertial sensor fusion: localization, mapping and sensor-to-sensor self-calibration. Int. J. Robot. Res. 30 (1), 56–79. https://doi.org/10.1177/0278364910382802.
Kramer, J.H., 2000. Digital mapping systems for field data collection. In: Proceedings of a Workshop on Digital Mapping Techniques: US Geological Survey, Open-file Report 00-325, pp. 13–19.
Kromer, R.A., Abellán, A., Hutchinson, D.J., Lato, M., Edwards, T., Jaboyedoff, M., 2015. A 4D filtering and calibration technique for small-scale point cloud change detection with a terrestrial laser scanner. Remote Sens. 7, 13029–13052. https://doi.org/10.3390/rs71013029.
Kurz, T.H., Buckley, S.J., Howell, J.A., Schneider, D., 2011. Integration of panoramic hyperspectral imaging with terrestrial lidar data. Photogramm. Rec. 26, 212–228. https://doi.org/10.1111/j.1477-9730.2011.00632.x.
Lee, S., Suh, J., Choi, Y., 2018. Review of smartphone applications for geoscience: current status, limitations, and future perspectives. Earth Sci. Inf. 11 (4), 463–486. https://doi.org/10.1007/s12145-018-0343-9.
Liang, J., Gong, J., Li, W., 2018. Applications and impacts of Google Earth: a decadal review (2006–2016). ISPRS J. Photogramm. Remote Sens. 146, 91–107. https://doi.org/10.1016/j.isprsjprs.2018.08.019.
Luetzenburg, G., Kroon, A., Bjørk, A.A., 2021. Evaluation of the Apple iPhone 12 Pro LiDAR for an application in geosciences. Sci. Rep. 11, 22221. https://doi.org/10.1038/s41598-021-01763-9.
Lundmark, A.M., Augland, L.E., Jørgensen, S.V., 2020. Digital fieldwork with fieldmove-how do digital tools influence geoscience students' learning experience in the field? J. Geogr. High. Educ. 44 (3), 427–440. https://doi.org/10.1080/03098265.2020.1712685.
Magri, L., Toldo, R., 2017. Bending the doming effect in structure from motion reconstructions through bundle adjustment. Int. Arch. Photogramm. Remote. Sens. Spat. Inf. Sci. XLII-2/W6, 235–241. https://doi.org/10.5194/isprs-archives-XLII-2-W6-235-2017.
McCaffrey, K.J.W., Jones, R.R., Holdsworth, R.E., Wilson, R.W., Clegg, P., Imber, J., Holliman, N., Trinks, I., 2005. Unlocking the spatial dimension: digital technologies and the future of geoscience fieldwork. J. Geol. Soc. 162 (6), 927–938. https://doi.org/10.1144/0016-764905-017.
McCarthy, A., Cosgrave, R., Meere, P., 2009. Use of the iPhone as a geological field tool: Practical benefits and technical limitations. In: EGU General Assembly Conference Abstracts, p. 11727.
Novakova, L., Pavlis, T.L., 2019. Modern Methods in Structural Geology of Twenty-first Century: Digital Mapping and Digital Devices for the Field Geology. In: Mukherjee, S. (Ed.), Teaching Methodologies in Structural Geology and Tectonics. Springer Geology, Singapore, pp. 43–54. https://doi.org/10.1007/978-981-13-2781-0_3.
Pavlis, T.L., Mason, K.A., 2017. The new world of 3D geologic mapping. GSA Today 27 (9), 4–10. https://doi.org/10.1130/GSATG313A.1.
Pavlis, T.L., Langford, R., Hurtado, J., Serpa, L., 2010. Computer-based data acquisition and visualization systems in field geology: results from 12 years of experimentation and future potential. Geosphere 6, 275–294. https://doi.org/10.1130/GES00503.1.
Penasa, L., Franceschi, M., Preto, N., Teza, G., Polito, V., 2014. Integration of intensity textures and local geometry descriptors from terrestrial laser scanning to map chert in outcrops. ISPRS J. Photogramm. Remote Sens. 93, 88–97. https://doi.org/10.1016/j.isprsjprs.2014.04.003.
Petroleum expert, 2021. FieldMove User Guide.
Pringle, J.K., Clark, J.D., Westerman, A.R., Stanbrook, D.A., Gardiner, A.R., Morgan, B.E.F., 2001. Virtual outcrops: 3-D reservoir analogues. Animations in Geology. J. Virtual Explor. 3, 1–6.
Pringle, J.K., Howell, J.A., Hodgetts, D., Westerman, A.R., Hodgson, D.M., 2006. Virtual outcrop models of petroleum reservoir analogues: a review of the current state-of-the-art. First Break 24, 33–42. https://doi.org/10.3997/1365-2397.2006005.
Pringle, J.K., Brunt, R.L., Hodgson, D.M., Flint, S.S., 2010. Capturing stratigraphic and sedimentological complexity from submarine channel complex outcrops to digital 3D models, Karoo Basin, South Africa. Pet. Geosci. 16, 307–330. https://doi.org/10.1144/1354-079309-028.
Reitman, N.G., Bennett, S.E., Gold, R.D., Briggs, R.W., DuRoss, C.B., 2015. High-resolution trench photomosaics from image-based modeling: workflow and error analysis. Bull. Seismol. Soc. Am. 105, 2354–2366. https://doi.org/10.1785/0120150041.
Roncella, R., Forlani, G., 2005. Extraction of planar patches from point clouds to retrieve dip and dip direction of rock discontinuities. ISPRS WG III/3, III/4, V/3 Workshop "Laser Scanning 2005". Enschede, the Netherlands, pp. 162–167.
Seers, T.D., Hodgetts, D., 2014. Comparison of digital outcrop and conventional data collection approaches for the characterization of naturally fractured reservoir analogues. Geol. Soc. Lond., Spec. Publ. 374, 51–77.
Seers, T.D., Hodgetts, D., 2016. Extraction of three-dimensional fracture trace maps from calibrated image sequences. Geosphere 12, 1323–1340. https://doi.org/10.1130/GES01276.1.
Seers, T.D., Sheharyar, A., Tavani, S., Corradetti, A., 2021. Virtual outcrop geology comes of age: the application of consumer-grade virtual reality hardware and software to digital outcrop data analysis. Comput. Geosci., 105006 https://doi.org/10.1016/j.cageo.2021.105006.
Senger, K., Nordmo, I., 2021. Using digital field notebooks in geoscientific learning in polar environments. J. Geosci. Educ. 69 (2), 166–177. https://doi.org/10.1080/10899995.2020.1725407.
Senger, K., Betlem, P., Birchall, T., Buckley, S.J., Coakley, B., Eide, C.H., Flaig, P.P., Forien, M., Galland, O., Gonzaga, L., Jensen, M., Kurz, T., Lecomte, I., Mair, K., Malm, R.H., Mulrooney, M., Naumann, N., Nordmo, I., Nolde, N., Ogata, K., Rabbel, O., Schaaf, N.W., Smyrak-Sikora, A., 2021. Using digital outcrops to make the high Arctic more accessible through the Svalbox database. J. Geosci. Educ. 69, 123–137. https://doi.org/10.1080/10899995.2020.1813865.
Snavely, N., Seitz, S.M., Szeliski, R., 2006. Photo tourism: Exploring photo collections in 3D. In: ACM Siggraph 2006 Papers, pp. 835–846.
Sun, Z., Sandoval, L., Crystal-Ornelas, R., Mousavi, S.M., Wang, J., Lin, C., et al., 2022. A review of earth artificial intelligence. Comput. Geosci. 105034 https://doi.org/10.1016/j.cageo.2022.105034.
Tavani, S., Granado, P., Corradetti, A., Girundo, M., Iannace, A., Arbués, P., Muñoz, J.A., Mazzoli, S., 2014. Building a virtual outcrop, extracting geological information from it, and sharing the results in Google Earth via OpenPlot and photoscan: an example from the Khaviz Anticline (Iran). Comput. Geosci. 63, 44–53. https://doi.org/10.1016/j.cageo.2013.10.013.
Tavani, S., Corradetti, A., Granado, P., Snidero, M., Seers, T.D., Mazzoli, S., 2019. Smartphone: an alternative to ground control points for orienting virtual outcrop models and assessing their quality. Geosphere 15 (6), 2043–2052. https://doi.org/10.1130/GES02167.1.
Tavani, S., Corradetti, A., Vinci, F., Parente, M., Mazzoli, S., Morsalnejad, D., Iannace, A., 2020a. Virtual geological mapping in the Lurestan region of the Zagros with Google Earth. Geological Field Trips and Maps 12, 1–11. https://doi.org/10.3301/GFT.2020.03.
Tavani, S., Pignalosa, A., Corradetti, A., Mercuri, M., Smeraglia, L., Riccardi, U., Seers, T.D., Pavlis, T., Billi, A., 2020b. Photogrammetric 3D model via smartphone GNSS sensor: workflow, error estimate, and best practices. Remote Sens. 12 (21), 3616. https://doi.org/10.3390/rs12213616.
Tibaldi, A., Bonali, F.L., Vitello, F., Delage, E., Nomikou, P., Antoniou, V., Becciani, U., de Vries, B.V.W., Krokos, M., Whitworth, M., 2020. Real world–based immersive virtual reality for research, teaching and communication in volcanology. Bull. Volcanol. 82, 1–12. https://doi.org/10.1007/s00445-020-01376-6.
Tiede, D., Lang, S., 2010. Analytical 3D views and virtual globes-scientific results in a familiar spatial context. ISPRS J. Photogramm. Remote Sens. 65, 300–307. https://doi.org/10.1016/j.isprsjprs.2009.12.002.
Uradziński, M., Bakuła, M., 2020. Assessment of static positioning accuracy using low-cost smartphone GPS devices for geodetic survey points' determination and monitoring. Appl. Sci. 10, 5308. https://doi.org/10.3390/app10155308.
van Veen, M., Hutchinson, D.J., Kromer, R., Lato, M., Edwards, T., 2017. Effects of sampling interval on the frequency-magnitude relationship of rockfalls detected from terrestrial laser scanning using semi-automated methods. Landslides 14, 1579–1592. https://doi.org/10.1007/s10346-017-0801-3.
Vasuki, Y., Holden, E.-J., Kovesi, P., Micklethwaite, S., 2014. Semi-automatic mapping of geological structures using UAV-based photogrammetric data: an image analysis approach. Comput. Geosci. 69, 22–32. https://doi.org/10.1016/j.cageo.2014.04.012.
Vaughan, A., Collins, N., Krus, M., Rourke, P., 2014. Recent development of an earth science app-FieldMove Clino. In: In EGU General Assembly Conference Abstracts, p. 14751.
Viseur, S., 2010. Automated Methods for Fully Exploring and Interpreting LIDAR Data Points. In: Proceedings of the EAGE Meeting. Barcelona, p. 4.

Walker, J.D., 2021. Geology in an Online World. GSA Today 31, 4–7 doi: GSATPrsAdrs20.1.
Walker, J.D., Tikoff, B., Newman, J., Clark, R., Ash, J.M., Good, J., Bunse, E.G., Möller, A., Kahn, M., Williams, R., Michels, Z., Andrew, J.E., Rufledt, C., 2019. StraboSpot data system for structural geology. Geosphere 15. https://doi.org/10.1130/GES02039.1.
Wallace, D.J., Witus, A.E., 2013. Integrating iPad technology in earth science K–12 outreach courses: field and classroom applications. J. Geosci. Educ. 61 (4), 385–395.
Wang, R., Lin, J., Li, L., Xiao, Z., Hui, Y., Xin, Y., 2021. A revised orientation-based correction method for SfM-MVS point clouds of outcrops using ground control planes with marks. J. Struct. Geol. 143, 104266 https://doi.org/10.1016/j.jsg.2020.104266.
Weng, Y.H., Sun, F.S., Grigsby, J.D., 2012. GeoTools: an android phone application in geology. Comput. Geosci. 44, 24–30. https://doi.org/10.1016/j.cageo.2012.02.027.
Whitmeyer, S.J., 2012. Community mapping in geology education and research: How digital field methods empower student creation of accurate geologic maps. In: Kastens, K.A., Manduca, C.A. (Eds.), Earth and Mind II: A Synthesis of Research on Thinking and Learning in the Geosciences: Geological Society of America Special Paper 486, pp. 171–174. https://doi.org/10.1130/2012.2486(27).
Whitmeyer, S.J., Nicoletti, J., De Paor, D.G., 2010. The digital revolution in geologic mapping. GSA Today 20 (4/5), 4–10. https://doi.org/10.1130/GSATG70A.1.
Whitmeyer, S.J., Pyle, E.J., Pavlis, T.L., Swanger, W., Roberts, L., 2019. Modern approaches to field data collection and mapping: Digital methods, crowdsourcing, and the future of statistical analyses. J. Struct. Geol. 125, 29–40. https://doi.org/10.1016/j.jsg.2018.06.023.
Whitmeyer, S.J., Atchison, C., Collins, T.D., 2020. Using mobile technologies to enhance accessibility and inclusion in field-based learning. GSA Today 30, 4–9. https://doi.org/10.1130/GSATG462A.1.
Wolniewicz, P., 2014. SedMob: a mobile application for creating sedimentary logs in the field. Comput. Geosci. 66, 211–218. https://doi.org/10.1016/j.cageo.2014.02.004.
Wu, C., 2011. VisualSFM: A Visual Structure from Motion System.
Xu, X., Aiken, C., Bhattacharya, J.P., Corbeanu, R.M., Nielsen, K.C., McMechan, G.A., Abdelsalam, M.G., 2000. Creating virtual 3-D outcrop. Lead. Edge 19, 197–202. https://doi.org/10.1190/1.1438576.
Yeon, Y.-K., 2021. KMapper: a field geological survey system. ISPRS Int. J. Geo-Inf. 10, 405. https://doi.org/10.3390/ijgi10060405.